

Synthesis of Dispersed Anatase Microspheres with Hierarchical Structures via Homogeneous Precipitation

Shaohong Liu,^[a] Xudong Sun,^{*[a]} Ji-Guang Li,^[a,b] Xiaodong Li,^[a] Zhimeng Xiu,^[a] and Di Huo^[a]

Keywords: Photochemistry / Nanostructures / Self-assembly / Titanium

Spherical anatase microparticles with good crystallinity have been synthesized by homogeneous precipitation under mild conditions (83–100 °C), employing ammonium fluotitanate as the titanium source and urea as the precipitant instead of more commonly used and highly reactive titanium sources such as titanium alkoxides and tetrachloride, which are sensitive to atmospheric moisture and therefore require special precautions. The as-prepared anatase particles were characterized by XRD, FE-SEM, UV/Vis spectroscopy, TG-DSC, and FTIR spectroscopy. The microspheres obtained in this work are hierarchically structured and are built up of rounded anatase nanocrystallites with a diameter of approxi-

mately 15–40 nm. The morphology of the nanoparticles within each microparticle changes from sphere to spindle as the reaction time is increased from 30 to 120 min in the experimental temperature range from 83 to 100 °C. A higher reaction temperature leads to enhanced growth of the nanocrystallites (primary particles) in solution and somewhat smaller anatase microspheres. The optical bandgaps and indirect bandgaps for all samples are approximately 3.23 and 2.95 eV, respectively, irrespective of their morphologies.

(© Wiley-VCH Verlag GmbH & Co. KGaA, 69451 Weinheim, Germany, 2009)

Introduction

Control over crystal structure, size, shape, and organization of titanium dioxide (TiO₂) nanomaterials has long been one of the main themes in TiO₂ research.^[1–5] TiO₂ nanomaterials with many different morphologies and crystal structures have been synthesized. For example, Chemseddine et al. have obtained uniform spherical and needle-like anatase nanoparticles with high crystallinity in a polycondensation reaction involving titanium alkoxides and tetramethylammonium hydroxide as starting materials and subsequent autoclave heating.^[2] Sugimoto et al. have prepared cuboidal and ellipsoidal TiO₂ nanoparticles by tuning the ratio of titanium isopropoxide (TIPO) and triethanolamine (TEOA).^[6] In the above two cases, tetramethylammonium hydroxide and TEOA were used as shape controllers, which adsorb on specific crystal planes of TiO₂ to tune the growth rate of these planes. TiO₂ nanorods have been prepared by dipping porous anodic alumina membranes (AAMs) into boiling TiO₂ sols followed by drying and heating. Differently sized anatase and rutile nanorods were produced with this technique, and each of these nano-

rods was found to be composed of TiO₂ nanoparticles and nanograins.^[7] TiO₂ nanowires and nanotubes have been classically obtained by autoclaving TiO₂ powers in a 10–15 M NaOH aqueous solution at 150–200 °C for 24–72 h without stirring.^[8] TiO₂ nanotubes have also been synthesized by many other methods, such as anodic aluminum oxide (AAO) templated growth via sol-gel^[9] and anodic oxidation.^[10,11] In these cases, the length and diameter of the TiO₂ nanotubes can be controlled over a wide range by modifying the processing parameters. Moreover, the phase-selective synthesis of TiO₂ nanocrystals (anatase, brookite, and rutile) has been achieved by Li et al. via a redox route under mild hydrothermal conditions (180 °C, 3 h), with titanium trichloride as the titanium source.^[12]

It has, however, proved rather difficult to prepare monodispersed TiO₂ microspheres of good dispersion and stability by direct hydrolysis of titanium alkoxides, primarily because the hydrolysis rate is too high to allow a separation of the nucleation and growth stages.^[13,14] By adding certain salts for electrostatic stabilization or polymeric stabilizers such as hydroxypropyl cellulose and block copolymers, many groups have been able to generate titania microspheres from titanium alkoxides in polar solvents.^[13,15] Ji-ang et al. and Yu et al. have demonstrated another route for the production of highly monodisperse titania particles involving hydrolysis of less reactive titanium precursors transformed from alkoxides.^[16,17] It should be noted that in most of the above studies the direct products are amorphous and thus a subsequent annealing at high temperatures

[a] Key Laboratory for Anisotropy and Texture of Materials (Ministry of Education), School of Materials and Metallurgy, Northeastern University, Shenyang, 110004, China
Fax: +86-24-23906316
E-mail: xdsun@mail.neu.edu.cn

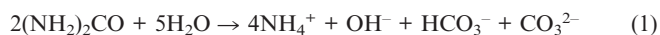
[b] Nano Ceramics Center, National Institute for Materials Science, Namiki 1-1, Tsukuba, Ibaraki, 305-0044, Japan

(e.g. 500 °C) is necessary for the crystallization of anatase or rutile microspheres. Recently, Li et al. obtained monodispersed crystalline spheres (ca. 154 nm) of brookite nanocrystals (ca. 25 nm) by treating a mixed solution of titanium trichloride and urea at temperatures below 100 °C.^[18] In this case, the slow oxidation of Ti³⁺ to Ti⁴⁺ ions by atmospheric oxygen, an appropriate solution pH, and the slow hydrolysis of urea seem to be crucial for the direct crystallization of brookite, a type of TiO₂ which is rarely obtained in a pure form.

The aforementioned studies all suggest that decreasing the reactivity of the titanium source should be an effective way of producing monodispersed TiO₂ microspheres. Therefore, instead of a highly reactive titanium source (titanium alkoxide or tetrachloride), which is likely to be sensitive to atmospheric moisture and therefore require special precautions, we have used ammonium fluorotitanate (AFT) in this work for TiO₂ synthesis. The urea homogeneous precipitation method has been used previously to prepare monodispersed spherical particles of several systems, such as ruthenium oxide,^[19] palladium,^[20] basic carbonate spheres of lanthanides,^[21] hydrated alumina,^[22] and hematite.^[23] We have managed to obtain both spherical and flower-like anatase-type TiO₂ particles of good crystallinity by homogeneous precipitation under mild conditions (83–100 °C), without the use of any additives, from aqueous solutions of AFT and urea by carefully controlling the synthetic parameters. The resultant powders have been characterized in detail by XRD, FE-SEM, TG-DSC, and FTIR and UV/Vis spectroscopy. We also propose formation mechanisms for the differently shaped anatase particles arising from investigations into the effects of the various processing parameters on the particle morphologies.

Results and Discussion

Urea decomposes at temperatures higher than about 80 °C during the urea precipitation process, as shown in Equation (1).



The NH₄⁺ and OH[−] ions generated then react readily with ammonium fluorotitanate to yield TiO₂ according to Equation (2).^[24]

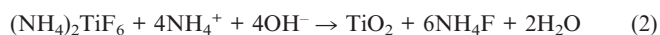


Table 1 summarizes the experimental parameters for particle synthesis and some properties of the products. Figure 1 shows XRD patterns for all the powders, from which it can be seen that the direct product is anatase-type TiO₂ (JCPDS, no. 01-071-1166) in each case, with no indication of any rutile or brookite impurity being detected. The sharp diffraction peaks suggest good crystallinity of the powders. In contrast to the traditional technique,^[24] which involves the transformation of γ-TiO₂ into anatase by calcination at 750 °C for 1 h, the method used in this work reduces the crystallization temperature to a very low one of 83–100 °C.

This enhanced crystallization may be attributed to the following two reasons: 1) the slow release of ammonia, which controls the rate of the precipitation reaction, by the forced hydrolysis of urea, and 2) the moderately high reaction temperature (83–100 °C) enhances the mobility of the configurational ions, thus enabling these ions to arrive at the correct positions for TiO₂ crystallization. The direct crystallization of pure anatase, rather than brookite or rutile, suggests the importance of the synthetic conditions, especially the solution pH (6–7 in this work) and supporting anions (F[−] and NH₄⁺ in this work) in the phase selection of TiO₂. Under similar processing conditions, the use of TiCl₃ solution as the titanium source yields pure brookite,^[18] while rutile tends to crystallize under highly acidic conditions.^[12]

Table 1. Synthetic conditions and crystallite sizes of the products.

Sample ID	Temp. (°C)	Time (min)	Crystallite size (nm)
S1	83	30	15.2
S2	90	30	21.9
S3	100	30	38.8
S4	83	120	33.6
S5	90	60	38.8
S6	90	120	38.8
S7	100	120	38.8

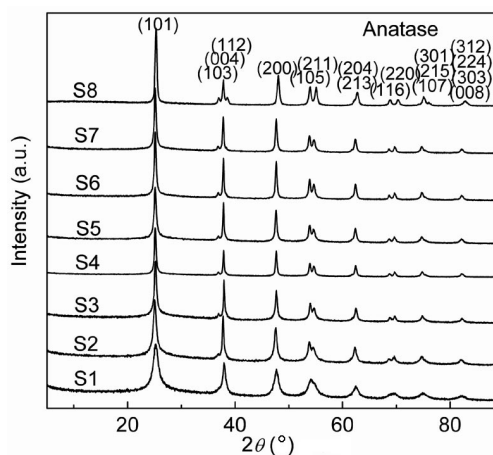


Figure 1. XRD patterns of the powders synthesized under various conditions. Labels S1–S7 correspond to the sample ID given in Table 1. Sample S8 was obtained by calcinating S2 at 570 °C for 2 h.

Figure 2 shows the particle morphologies of the powders obtained after 30 min at three typical temperatures of 83 (sample S1, Figure 2, a), 90 (S2, Figure 2, b,c), and 100 °C (S3, Figure 2, d). The resultant particles are microspheres in each case, irrespective of the reaction temperature. Furthermore, these microparticles show good dispersion and no apparent aggregation is observed. Some researchers have also prepared anatase microspheres by a one-step synthetic method. Liu et al., for example, have used TiCl₃ as the titanium source to prepare anatase microspheres in a hydrothermal method by heating at 90 °C for 24 h.^[25] Similarly, Yu et al. have used Ti(SO₄)₂ as the titanium source to prepare anatase microspheres in a chemically induced self-transformation method by heating at 160 °C for about

6 h.^[26] The diameter of the anatase microspheres is roughly 700–800 nm for S1, though some even smaller spheres were occasionally found (Figure 2, a). A higher reaction temperature leads to somewhat smaller anatase microspheres, with average sizes for samples S2 (Figure 2, b) and S3 (Figure 2, d) of around 600 and 500 nm, respectively. The rough particle surfaces, however, indicate the existence of substructures within each microsphere, as also evidenced by high magnification FE-SEM observation of sample S2 (Figure 2, c), where rounded primary nanoparticles are clearly seen. The average crystallite sizes were determined from the (101) XRD peaks by applying the Scherrer formula (Table 1). Obviously, a higher temperature leads to enhanced growth of the nanocrystallites (primary particles) in solution. Such a hierarchical microstructure is similar to that observed from monodispersed brookite submicron spheres.^[18] The anatase microspheres obtained in this work are apparently formed by an aggregation mechanism, or, in other words, a surface-energy-driven self-assembly. Nanoparticles are generated via precipitation by nucleation and growth at the very beginning of the reaction. As the number of nanoparticles increases, the total surface energy of the nanoparticles in solution increases accordingly, and thus the primary particles assemble into microspheres in order to reduce the total surface energy. Raising the synthesis temperature enhances the random movements of the primary particles (building units) in solution, thereby hindering their aggregation and leading to a decreased average size of the microspheres at a higher reaction temperature.

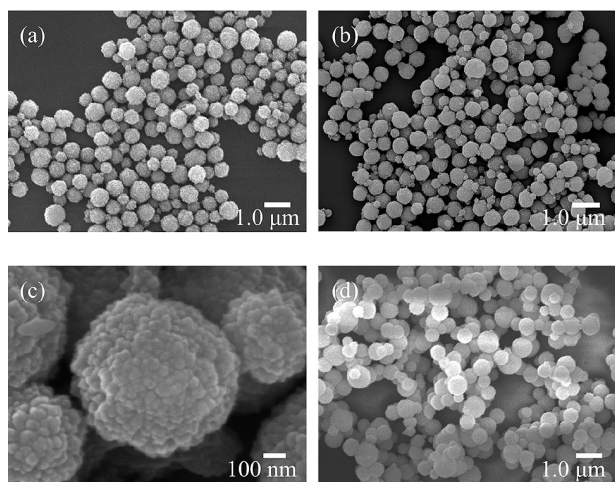


Figure 2. FE-SEM micrographs showing the particle morphologies of samples S1 (a), S2 (b,c), and S3 (d).

The reaction time was found to be a decisive factor affecting the morphology of the final particles (Figure 3). Sample S1 undergoes significant morphological changes at 83 °C when prolonging the reaction time from 30 to 120 min. Considering the crystallite growth (Table 1) during this additional aging period of 90 min, it was found that the fine spherical nanoparticles (building units) within each microsphere (Figure 2, a) evolve through growth into spindles, which leads to the collapse of the microsphere and the formation of small flowerlike particles composed of spin-

dles along with some discrete spindle-like particles (Figure 3, a). Such a scenario was evidenced by the time-course morphology evolution of the particles synthesized at 90 °C for 30 (S2, Figure 2, b), 60 (S5, Figure 3, b), and 120 min (S6, Figure 3, c). A similar morphological evolution was also observed for sample S3 at an even higher temperature of 100 °C, with the powder produced after 120 min of reaction (S7, Figure 3, d) showing a general morphology similar to that of S6 (Figure 3, c), although the aggregates are finer.

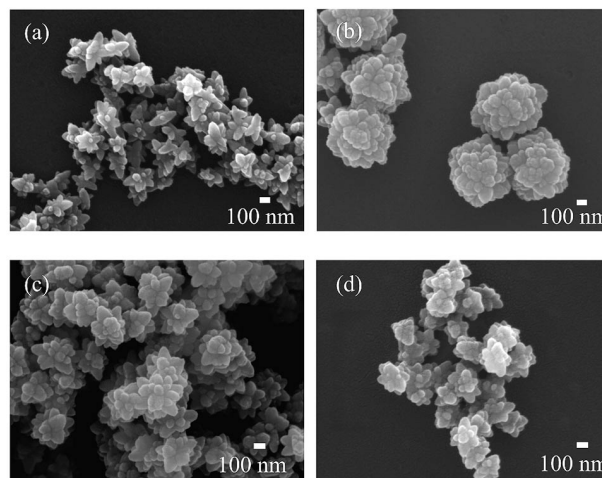


Figure 3. FE-SEM micrographs showing the particle morphologies of samples S4 (a), S5 (b), S6 (c), and S7 (d).

UV/Vis absorption spectroscopy was used to determine the indirect interband transition energies for three typical powders (samples S2, S4, and S6); the results are shown in Figures 4 and 5. The optical absorption edges were found to be 384.2 nm for all three samples, which corresponds to an optical bandgap of around 3.23 eV. The optical bandgaps of anatase have been widely reported, and the values determined in this work are in excellent agreement with the literature ones (ca. 3.2 eV for anatase).^[27] TiO₂ is known to be an indirect semiconductor,^[28,29] for which the relation between absorption coefficient (α) and incident photon energy ($h\nu$) can be written as $\alpha = B_i (h\nu - E_g)^2/h\nu$,

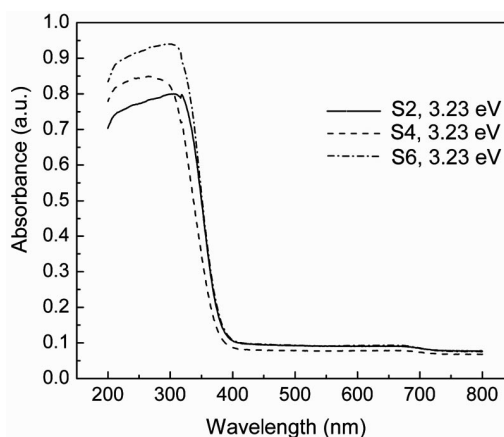


Figure 4. Typical UV/Vis absorption spectra of the as-prepared powders.

where B_i is the absorption constant for indirect transitions.^[30,31] Plots of $(Ah\nu)^{1/2}$ vs. $h\nu$ from the spectroscopic data in Figure 4 are shown in Figure 5. Extrapolating the linear parts of the curves gives an indirect bandgap of around 2.95 eV for all three samples, which is very close to the calculated value of 2.91 eV corresponding to the $X_{1a} \rightarrow G_{1b}$ indirect interband transition of TiO_2 .^[32]

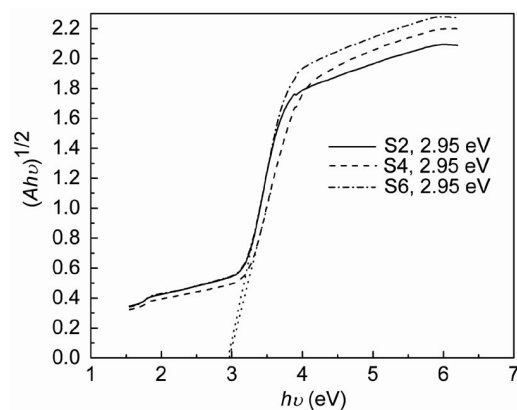


Figure 5. Determination of the indirect interband transition energies for as-prepared samples S2, S4, and S6. A in the label on the y -axis represents absorbance, which is proportional to the absorption coefficient α .

The thermal behavior of the anatase microspheres was investigated using sample S2 as an example, and the results are shown in Figure 6. The TG curve recorded under a flow of nitrogen gas shows significant weight losses (up to ca. 20%) in the temperature range 25–1000 °C, which are mainly due to the removal of adsorbed substances and dehydration of the as-prepared anatase. The broad exotherm recorded at about 570 °C might be due to the enhanced crystallization of anatase rather than an anatase \rightarrow rutile phase transition. This proposal was supported by XRD analysis of S8 obtained upon calcining S2 at 570 °C for 2 h (Figure 1).

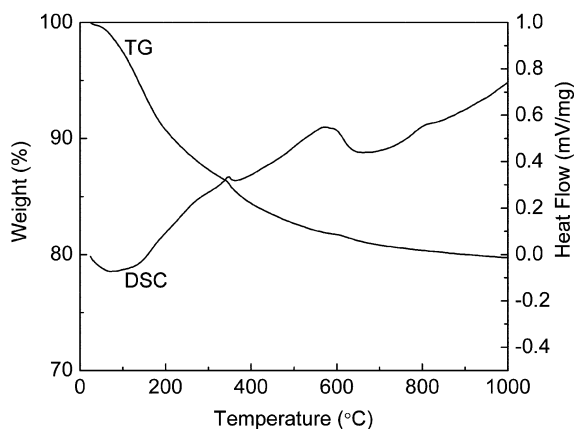


Figure 6. TG-DSC curves for sample S2.

The fact that the as-synthesized anatase is hydrated was confirmed by the appearances of strong absorption bands at around 1640 (the O–H bending mode) and 3300 cm^{-1} (the O–H stretching mode) in the FTIR spectrum (Fig-

ure 7). The absorption bands at about 1400 and 3166 cm^{-1} may suggest the presence of some ammonium ions arising from the starting titanium source and urea hydrolysis. As XRD analysis (Figure 1) only suggests the presence of anatase-type TiO_2 in the products, it is reasonable to assume that these ammonium ions might arise from some impurities adsorbed on the TiO_2 surfaces. The absorption band at around 580 cm^{-1} corresponds to the Ti–O stretching mode. All the above observations are consistent with the literature.^[33]

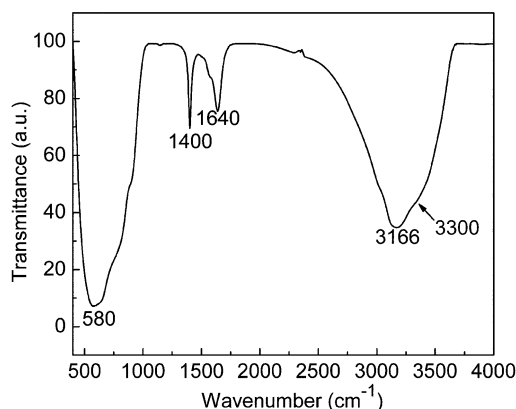


Figure 7. FTIR spectrum of sample S2.

Conclusions

Crystalline anatase microspheres with hierarchical structures have been directly obtained via homogeneous precipitation under mild conditions (83–100 °C, 30–120 min) with ammonium fluorotitanate as the titanium source and urea as the precipitant. The morphology of the nanoparticles within each microparticle changes from spherical to spindle-shaped as the reaction time is increased from 30 to 120 min. A higher reaction temperature leads to enhanced growth of the nanocrystallites (primary particles) in solution and somewhat smaller anatase microspheres. The optical bandgaps of all samples were determined to be around 3.23 eV and the indirect bandgaps around 2.95 eV, irrespective of their morphologies.

Experimental Section

Particle Synthesis: The titanium source in this paper is ammonium fluorotitanate $[(\text{NH}_4)_2\text{TiF}_6]$, AFT, Reagent grade, Sinopharm Chemical Reagent Co., Ltd.]. Although ammonium hydroxide has been widely used as a precipitant, it reacts with AFT immediately to give nongelatinous $\gamma\text{-TiO}_2$ of an amorphous nature.^[24] To control the precipitation reaction, urea $[\text{CO}(\text{NH}_2)_2]$, reagent grade, Sinopharm Chemical Reagent Co., Ltd.], which is known to release ammonia slowly by forced hydrolysis at temperatures above around 83 °C, was used instead of ammonium hydroxide. All chemicals were used as received without further purification. For powder synthesis, the desired amounts of AFT and urea were mixed together and diluted with distilled water to the intended concentrations of 0.015 M for AFT and 0.5 M for urea during the preparation of all

samples in our work. To speed up heating, a beaker containing 800 mL of the thus-made solution was sealed with a preservative film, and a thermometer was inserted into the solution through a hole in the film to measure the solution temperature. The as-prepared solution was then heated under magnetic stirring to the intended temperature and held there for a certain period of time (Table 1). After cooling naturally to room temperature, the resultant solids were recovered by centrifugation, washed with distilled water by ultrasonication and centrifuge, and finally dried at 60 °C for 5 h.

Characterization Techniques: Phase identification was performed by X-ray diffractometry (XRD) with a Philips PW3040/60 diffractometer (Philips, Eindhoven, The Netherlands) operating at 40 kV/40 mA using nickel-filtered Cu- K_{α} radiation. The particle morphology was observed by field emission scanning electron microscopy (FE-SEM, Model JSM-7001F, Oxford instrument HKL) at 15 kV. Thermogravimetry-differential scanning calorimetry (TG-DSC) analysis of the product was performed under flowing nitrogen (10 mL/min) with an STA 409 PC/PG analyzer (Netzsch, Germany) at a heating rate of 5 °C/min. FTIR spectroscopy (Spectrum RXI, Perkin-Elmer, Shelton, CT) of the powders was performed by the standard KBr method. The UV/Vis absorption spectra of the powders were recorded using a Lambda750 spectrometer (Perkin-Elmer, Shelton, CT) with a 60-mm integrating sphere.

Acknowledgments

This work was supported by the National Natural Science Fund for Distinguished Young Scholars (50425413), the Program for New Century Excellent Talents in University (NCET-25-0290), the National Natural Science Foundation of China (50672014), and the Program for Changjiang Scholars and Innovative Research Teams in University (PCSIRT, IRT0713).

- [1] X. B. Chen, S. S. Mao, *Chem. Rev.* **2007**, *107*, 2891–2959.
- [2] A. Chemseddine, T. Moritz, *Eur. J. Inorg. Chem.* **1999**, 235–245.
- [3] Y.-W. Jun, M. F. Casula, J.-H. Sim, S. Y. Kim, J. Cheon, A. P. Alivisatos, *J. Am. Chem. Soc.* **2003**, *125*, 15981–15985.
- [4] M. Kolář, H. Měšťánková, J. Jirkovský, M. Heyrovský, J. Šubrt, *Langmuir* **2006**, *22*, 598–604.
- [5] A. S. Barnard, P. Zapol, L. A. Curtiss, *J. Chem. Theory Comput.* **2005**, *1*, 107–116.
- [6] T. Sugimoto, X. P. Zhou, A. Muramatsu, *J. Colloid Interface Sci.* **2003**, *259*, 53–61.
- [7] L. Miao, S. Tanemura, S. Toh, K. Kaneko, M. Tanemura, *J. Cryst. Growth* **2004**, *264*, 246–252.
- [8] Y. X. Zhang, G. H. Li, Y. X. Jin, Y. Zhang, J. Zhang, L. D. Zhang, *Chem. Phys. Lett.* **2002**, *365*, 300–304.
- [9] S. M. Liu, L. M. Gan, L. H. Liu, W. D. Zhang, H. C. Zeng, *Chem. Mater.* **2002**, *14*, 1391–1397.
- [10] V. Zwillig, E. Darque-Ceretti, A. Boutry-Forveille, D. David, M. Y. Perrin, M. Aucouturier, *Surf. Interface Anal.* **1999**, *27*, 629–637.
- [11] O. K. Varghese, D. Gong, M. Paulose, K. G. Ong, E. C. Dickey, C. A. Grimes, *Adv. Mater.* **2003**, *15*, 624–627.
- [12] J.-G. Li, T. Ishigaki, X. Sun, *J. Phys. Chem. C* **2007**, *111*, 4969–4976.
- [13] S. Eiden-Assmann, J. Widoniak, G. Maret, *Chem. Mater.* **2004**, *16*, 6–11.
- [14] W. P. Hsu, R. Yu, E. Matijević, *J. Colloid Interface Sci.* **1993**, *156*, 56–65.
- [15] J. H. Jean, T. A. Ring, *Colloids Surf.* **1988**, *29*, 273–291.
- [16] X. Jiang, T. Herricks, Y. Xia, *Adv. Mater.* **2003**, *15*, 1205–1209.
- [17] H. K. Yu, G.-R. Yi, J.-H. Kang, Y.-S. Cho, V. N. Manoharan, D. J. Pine, S.-M. Yang, *Chem. Mater.* **2008**, *20*, 2704–2710.
- [18] J.-G. Li, C. Tang, D. Li, H. Haneda, T. Ishigaki, *J. Am. Ceram. Soc.* **2004**, *87*, 1358–1361.
- [19] F. Porta, W. P. Hsu, E. Matijević, *Colloids Surf.* **1990**, *46*, 63–74.
- [20] S. Kratochvil, E. Matijević, *J. Mater. Res.* **1994**, *9*, 2404–2410.
- [21] a) E. Matijević, W. P. Hsu, *J. Colloid Interface Sci.* **1987**, *118*, 506–523; b) D. Sordet, M. Akinc, *J. Colloid Interface Sci.* **1988**, *122*, 47–59; c) W. P. Hsu, G. Wang, E. Matijević, *Colloids Surf.* **1991**, *61*, 255–267.
- [22] a) T. Tsuchida, S. Kitajima, *J. Mater. Sci.* **1992**, *27*, 2713–2718; b) T. Tsuchida, S. Kitajima, *Chem. Lett.* **1990**, 1769–1772.
- [23] D. Daichuan, H. Pinjie, D. Shushan, *Mater. Res. Bull.* **1995**, *30*, 531–535.
- [24] T. Moeller, in *Inorganic Synthesis*, vol. V (Eds.: G. H. Cady, E. G. Rochow, H. F. Holtzclaw, W. C. Schumb, J. Kleinberg, J. D. Scott), McGraw-Hill Book Company, **1957**, p. 81.
- [25] L. Liu, H. Liu, Y.-P. Zhao, Y. Wang, Y. Duan, G. Gao, M. Ge, W. Chen, *Environ. Sci. Technol.* **2008**, *42*, 2342–2348.
- [26] J. Yu, S. Liu, M. Zhou, *J. Phys. Chem. C* **2008**, *112*, 2050–2057.
- [27] M. R. Hoffmann, S. T. Martin, W. Y. Choi, D. W. Bahnemann, *Chem. Rev.* **1995**, *95*, 69–96.
- [28] C. Kormann, D. W. Bahnemann, M. R. Hoffmann, *J. Phys. Chem.* **1988**, *92*, 5196–5201.
- [29] M. M. Rahman, K. M. Krishna, T. Soga, T. Jimbo, M. Umeno, *J. Phys. Chem. Solids* **1999**, *60*, 201–210.
- [30] A. Hagfeldt, M. Graetzel, *Chem. Rev.* **1995**, *95*, 49–68.
- [31] J. C. Yu, J. G. Yu, W. K. Ho, Z. T. Jiang, L. Z. Zhang, *Chem. Mater.* **2002**, *14*, 3808–3816.
- [32] N. Daude, C. Gout, C. Jouanin, *Phys. Rev. B* **1977**, *15*, 3229–3235.
- [33] K. Nakamoto, *Infrared and Raman Spectra of Inorganic and Coordination Compounds*, 4th ed., John Wiley & Sons, **1997**.

Received: October 8, 2008

Published Online: February 4, 2009